Available online at www.CivileJournal.org

Civil Engineering Journal

(E-ISSN: 2476-3055; ISSN: 2676-6957)

Vol. 11, No. 11, November, 2025

Insights Into the Load-Carrying Mechanism and Interactive Effects of Dissimilar Piles in Cushioned Piled Rafts

Bantayehu Uba Uge [1, 2], Yuancheng Guo [1*], Jun Zhao [1], Yunlong Liu [1*], Mudassir Mehmood [3, 4], Chenyu Lv [5], Yanyan Xia [6]

[1] *Department of Civil Engineering, Zhengzhou University, Zhengzhou 450001, China.*

[2] *School of Civil Engineering, Hawassa University, Hawassa, Ethiopia.*

[3] *State key laboratory of Metal Mining Safety and Disaster Prevention and Control, Maanshan Anhui 243000, China.*

[4] *School of Resources and Safety Engineering, Chongqing University, Chongqing 400044, China.*

[5] *Department of Civil Engineering, Henan University of Engineering, Zhengzhou 451191, China.*

[6] *Department of Water Resources and Transportation, Zhengzhou University, Zhengzhou 450001, China.*

Received 18 August 2025; Revised 11 October 2025; Accepted 14 October 2025; Published 01 November 2025

Abstract

Disconnecting pile heads from the raft has gained wide application because the gravel and geogrid layers filling the space between them create a more even pressure distribution and reduce differential settlement. However, due to the complexity of modelling the multiple interfaces in the superstructure-foundation-subsoil system, previous findings on load-transfer mechanisms, interaction effects, and group optimization remain incomplete. Moreover, the common analytical approach employed for understanding the load transfer mechanism is the "unit cell' concept, which cannot fully capture dissimilarity in the group. To address these limitations, this study aims to develop an analytical framework for predicting the load-settlement response of cushioned piled rafts with dissimilar piles. The proposed method simplifies the cushion-pile-soil interaction using a Winkler-type Spring model, while a hyperbolic load-transfer function captures the nonlinear pile-soil behavior. The model was verified against existing experimental and showed close agreement. It successfully captured the load-sharing mechanism, confirming that stiffer, longer, or larger-diameter piles attract a disproportionately higher share of the load. The novelty of this work lies in the establishment of an analytical model based on the principles of dissimilar pile groups but extended to include cushion force transmission, a critical integration that provides a realistic tool for practice.

Keywords: Disconnected Piled Raft; Dissimilar Piles; Load Transfer Approach; Cushion; Soil-Structure Interaction.

1. Introduction

Identical piles are commonly used to transmit the superstructure load of tall buildings to the ground, partly due to simplicity and predictability [1, 2]. While this ensures the use-safety requirements, the optimization of the pile group is often necessary to compensate for material requirements and installation costs [3, 4]. More specifically, rafts supported by few piles can be strategically installed to take advantage of the load-carrying performance of both the piles and the raft itself in challenging ground conditions. The geoengineering community has long recognized the use of such settlement-reducing piles, a concept dating back to the late 1970s [5], which has shifted the design approach towards realizing admissible settlement rather than merely achieving the desired load-bearing capacity [6]. Unlike the

* Corresponding author: guoyc@zzu.edu.cn; liuyunlong@zzu.edu.cn

http://dx.doi.org/10.28991/CEJ-2025-011-11-01

conventional pile groups, piled rafts share the load with the surrounding soil [7, 8]. This leads to key interactions characterized by raft-cushion (or soil, if the piles are connected) and soil-pile interface properties, involving four main interaction types: soil-soil, cushion-pile-soil, pile-soil-pile, pile-soil-raft (for connected piled rafts), soil-cushion-raft, and pile-cushion-raft for detached piled rafts, as shown in Figure 1. Regardless of the piles' attachment to the raft, the foundation system behaves as a unit to resist the imposed superstructure load.

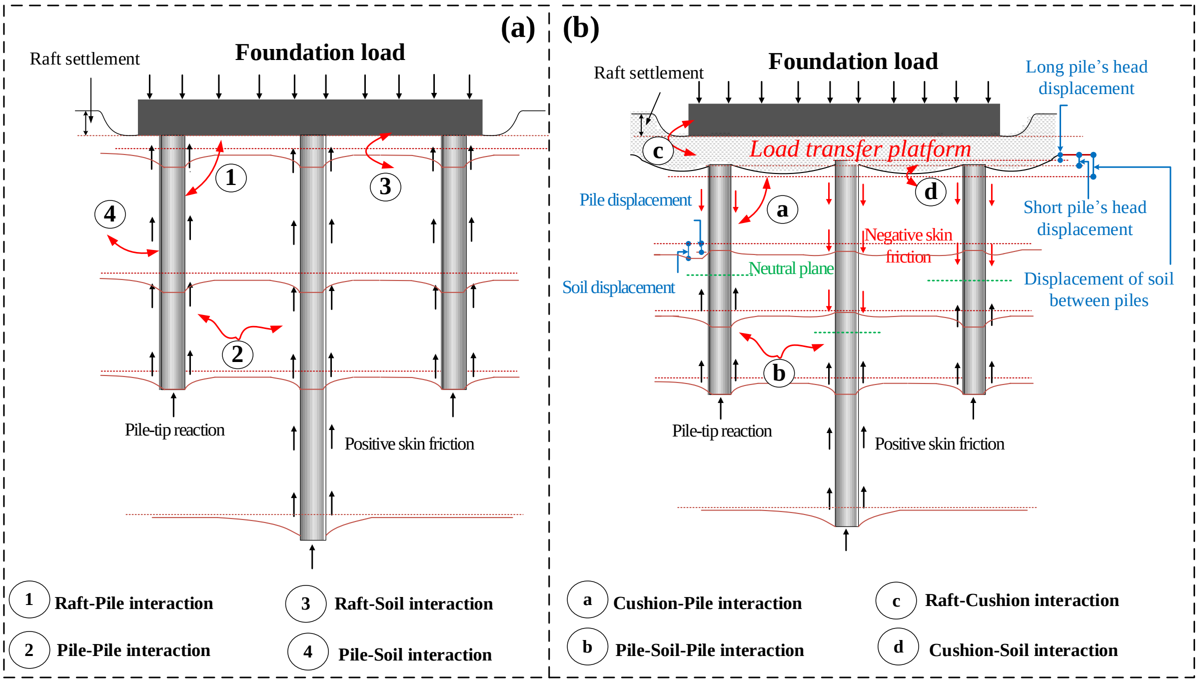

Figure 1. Typical interaction in (a) connected and (b) unconnected piled-raft with unequal pile lengths (Modified after Uge et al. [9])

The inherent complexity of piled rafts is further intensified by real-world conditions that frequently necessitate the use of dissimilar piles with varying geometry and stiffness. Spatial variability in natural soil deposits, site constraints from existing infrastructure, and non-uniform superstructure loading all demand targeted resistance that identical pile groups cannot provide efficiently [10–12]. For instance, core zones with heavy columns, elevator shafts, or mechanical equipment demand higher bearing capacity than peripheral areas. Consequently, a growing body of research demonstrates the benefits of strategically using non-uniform pile configurations. Liu et al. [13] experimentally observed that larger-diameter piles under high-load zones mobilized greater shaft friction and base resistance, while smaller piles acted as load stabilizers, reducing stress concentrations. According to the numerical analysis results of Zhang et al. [4], pile groups with longer central piles and shorter edge piles not only reduced differential settlement but also optimized material usage without sacrificing performance. Moreover, non-uniform arrangements, particularly those with longer or stiffer piles strategically placed at corners or high-moment zones, offer enhanced rotational resistance and inertial effects by improving stiffness distribution. Such pile groups with varied stiffness and spatial layout reduce base shear and moment demands on the superstructure, allowing for better load redistribution and minimized rocking effects during seismic events [14–16].

Interestingly, the literature on the geometric and material nonlinearity of piled raft systems has evolved from foundational simplifications to models that are sophisticated enough to embrace heterogeneity not just as a challenge but as a critical design parameter. Accordingly, previous studies have significantly advanced our understanding of how dissimilar piles engage themselves with the surrounding soil at different depths, demonstrating that stiffer piles receive a higher proportion of the foundation load [13, 17]. However, there is a dearth of studies on available analytical tools for practice. The common "unit cell" concept, often employed to simplify the analysis of load transfer, cannot capture the essential dissimilarity within a pile group [18, 19]. While sophisticated nonlinear 3D numerical methods offer a more realistic representation [20, 21], they are often too complex for routine design and preliminary optimization. Moreover, prior research on disconnected piled rafts has been constrained by these simplified approaches or has focused predominantly on experimental and numerical analysis of load transfer from the raft to the pile head [22, 23], overlooking the integrated analytical modelling of the complex cushion-pile-soil interaction in groups with dissimilar piles.

In response to these challenges, this paper establishes a computational model to quantify the load-carrying characteristics of cushioned piled rafts comprising dissimilar piles. The model formulation is established based on the iterative approaches developed for dissimilar pile groups [24] and is extended to integrate a physical representation of the cushion effect. By integrating two key components into a single, practice-oriented tool, this work presents a novel solution that bridges the gap between overly simplified concepts and complex numerical models. First, the cushion-pile-soil interaction is simplified through a Winkler-type spring model, which facilitates load transfer between the raft and the pile-soil system [25]. Second, the nonlinear pile-soil interactive behavior for each dissimilar pile is represented by a hyperbolic load-transfer function [26, 27], capturing the progressive mobilization of shaft and base resistance. By doing so, the model can simulate the complex interaction between long and short piles, as well as piles of different diameters, while taking into consideration the stress redistribution role of the cushion layer. The proposed computational model was verified against existing experimental data from the literature [13, 28], with which it compared favorably. The remainder of this paper is structured as follows: Section 2 provides a detailed classification and discussion of the various types of dissimilarity in piles (length, diameter, stiffness, and configuration). Section 3 presents a comprehensive discussion on the interactive effects, detailing the developed analytical methodology, the governing equations, and the proposed computation algorithm, as shown in Figures 2b and 2c. Finally, Section 4 summarizes the key insights derived from the analysis and outlines directions for future research.

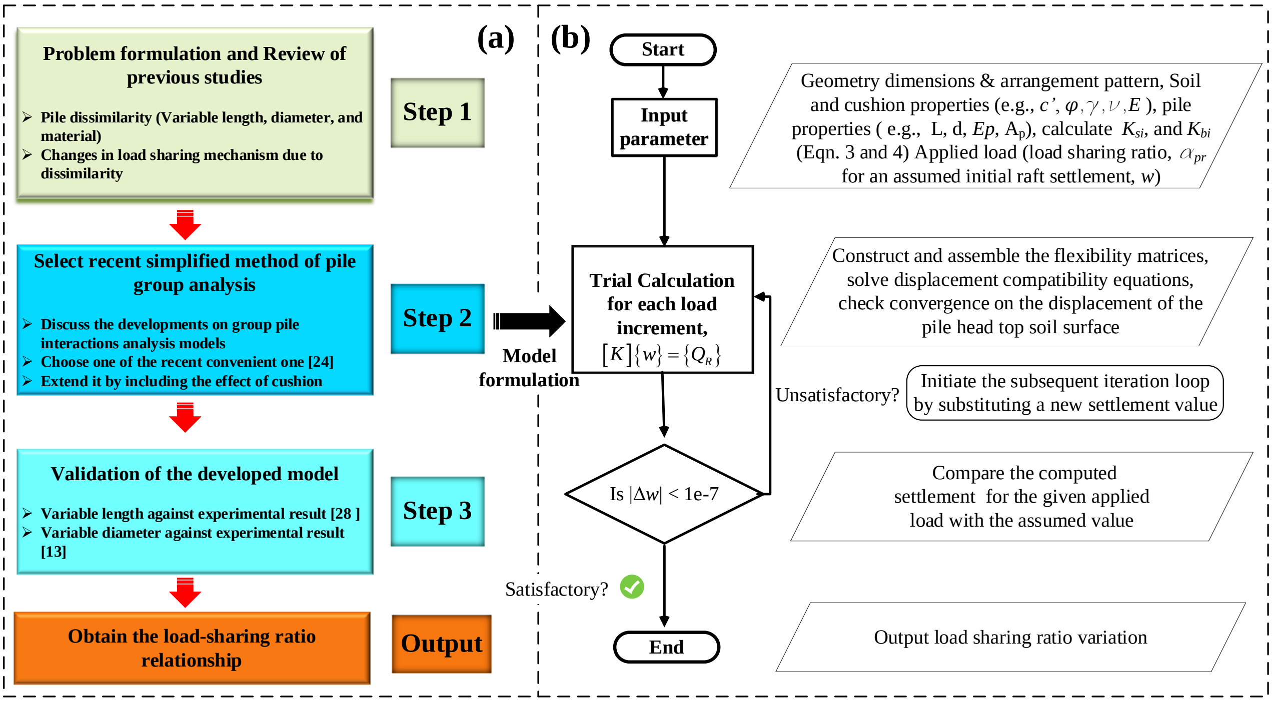

Figure 2. Flowchart of (a) research methodology, and (b) model computation algorithm

2. Dissimilarity in Piles

Over the ensuing years, pile geometric differences and dissimilarities in material properties have been intentionally introduced, either during the design phase or through the reuse of existing foundation piles, to achieve economic benefits [3, 29]. With numerous design factors to consider (e.g., cushion thickness and stiffness, raft geometric dimensions, pile geometric dimensions and stiffness, etc.), a wide range of designs is possible, allowing the designer to choose one at random or with limited expertise. Therefore, attentively designed dissimilarity with optimum pile arrangement is a way forward in engineering practice to fully mobilize the bearing capacity of individual piles and to diminish angular distortion and differential foundation settlement [30, 31]. Nonetheless, it should be noted that the use of dissimilar piles may also introduce significant risks of differential settlement and uneven load distribution if not properly analyzed and designed.

2.1. Dissimilarity in Length

In the last several years, unequal length piles (i.e., a group with short and long piles) have been extensively employed in infrastructure projects to attack static and dynamic loads imposed on infrastructures [32, 33]. Accordingly, several studies have been conducted under various loading scenarios, viz., vertical loading [25], eccentric loading [34], lateral loading [29, 35], passive loading [36], and combined static and dynamic loading [16, 37]. Such studies have disclosed that longer piles attract a disproportionately higher share of the load due to their higher stiffness and greater surface area for shaft resistance and end-bearing capacity, as shown in Figure 3. Accordingly, groups with varying pile lengths demonstrate a tendency for longer piles to dominate load redistribution, while shorter piles contribute less significantly and get protected by the long piles [38]. Sometimes the short piles remain underutilized since they may not mobilize their full capacity. This has led to implementing rigid long and flexible short piles to avoid inefficient use of materials [39–41]. Consequently, dissimilarity in pile length is usually strategically combined with variations in stiffness. In such systems, long, rigid piles collaborate with short, flexible ones within the upper soil strata, where the shorter piles primarily serve to increase the overall bearing capacity of the foundation.

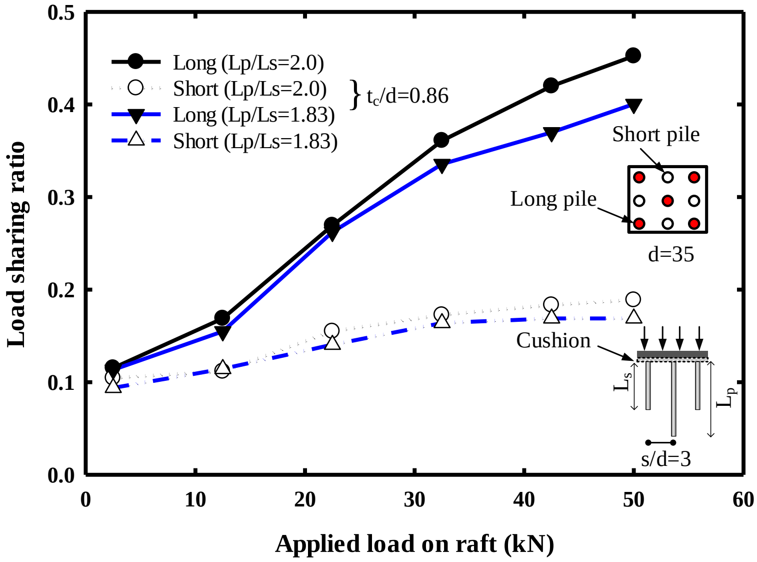

Figure 3. Comparison of the load sharing ratio variation over long and short pile heads in disconnected piled rafts subjected to vertical loading (Modified after Pengfei et al. [17])

Moreover, the interaction between piles of varying lengths within a disconnected piled raft foundation constitutes a highly complex soil-structure interaction (SSI) problem. This complexity arises from several interdependent factors, such as integrating components with vastly different stiffness characteristics, viz., the rigid raft, the cushion, the long piles, the short piles, and the surrounding soil. The proportion of load carried by the soil (transferred from the raft through the cushion layer), the long piles, and the short piles is not static. It continuously redistributes under changing structural or seismic loads, which creates a dynamic and interdependent system. While dissimilarity in length engages soil strata at different depths, a parallel and often complementary strategy involves varying the pile cross-section. Dissimilarity in diameter directly alters the pile's axial stiffness and load-attraction capacity from the outset.

2.2. Dissimilarity in Diameter

The cushion-pile-soil-raft-structure interaction in a disconnected piled raft foundation also becomes significantly more intricate when the system incorporates piles of dissimilar diameters. Due to the cross-sectional dissimilarity, the load distribution mechanism is fundamentally altered in which stiffer elements, typically the larger-diameter piles, attract a disproportionate share of the load, as shown in Figure 4. This is due to their greater cross-sectional area (i.e., higher axial stiffness) and larger surface area (i.e., corresponding to the shear stiffness), which leads to a higher zone of stress influence and pile-soil stress ratio [13]. Consequently, in a similar manner with the response of varying lengths, the larger piles may mobilize their ultimate capacity or experience higher stresses, while smaller diameter piles may remain underutilized. According to Tong et al. [42], the cushion thickness to pile diameter ratio (t_c/d) acts as a primary control mechanism to mediate and optimize stress redistribution between the rigid raft, the piles, and the underlying soil. This function becomes critically important when incorporating varying diameter piles (e.g., in long-short pile systems), as a uniform ratio fails to simultaneously mobilize the full bearing capacity of all components.

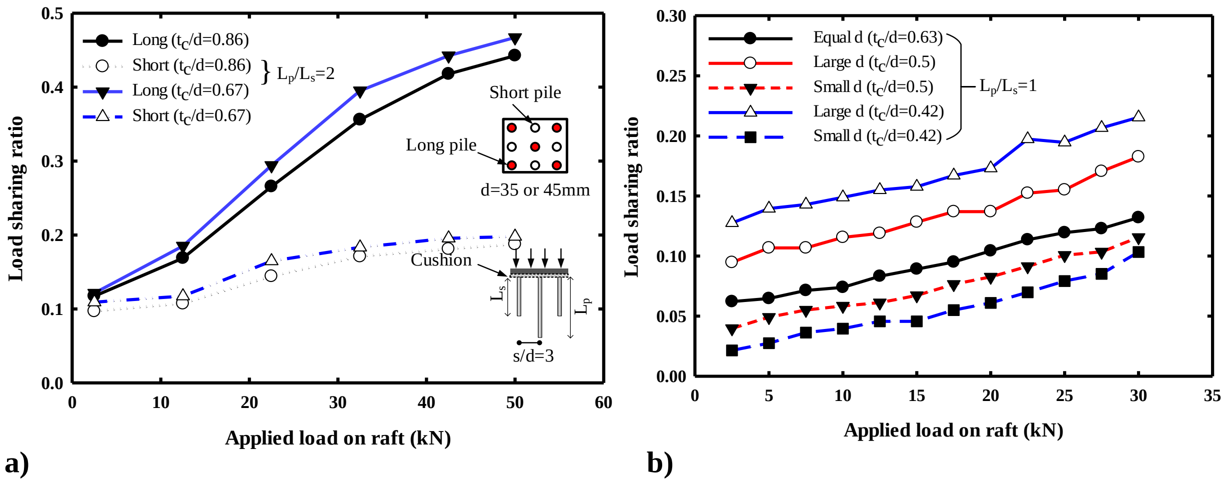

Figure 4. Comparison of the load sharing ratio variation over (a) long and short pile heads [17], and (b) equal length pile heads [13] due to pile cross-sectional dissimilarity in disconnected piled rafts subjected to vertical loading

2.3. Dissimilarity in Stiffness

The preceding discussion on length and diameter inherently introduces the overarching concept of dissimilarity in stiffness, as both geometric properties are primary determinants of a pile's flexural and axial rigidity. This subsection explicitly examines cases where stiffness variation is directly engineered through material choice or composite design. In most cases, pile stiffness variations during design have been introduced along with length dissimilarities to optimize the load-settlement behavior of composite foundations, as explained above. Accordingly, several studies have dealt with long rigid and short flexible piles in the group [39, 40, 43–45]. Yang & Zhang [46] demonstrated that dissimilarities in pile length and stiffness fundamentally alter the superstructure-foundation interaction by shifting a greater portion of the axial load and negative skin friction to the longer, stiffer piles, though this effect diminishes beyond a certain length. Jais et al. [47] demonstrated that stone columns (flexible piles) used in conjunction with rigid concrete piles under a raft foundation reduced total settlement by up to 27% and improved load-sharing efficiency.

Similarly, Fang et al. [48] explored the use of biocemented coral sand piles (BCS piles) as flexible elements in a long-short pile composite system, reporting an up to 68% increase in bearing capacity and more uniform stress distribution compared to untreated ground. According to the static load test of Zhang et al. [49], rigid plain concrete piles gained more load sharing due to their significantly higher stiffness, which allowed them to attract and transfer a greater proportion of the applied load compared to the more compliant flexible piles (soil compaction piles) of similar geometric dimensions, as shown in Figure 5. The study also concluded that negative skin friction did not develop along the flexible piles because their modulus was very close to that of the surrounding improved soil, resulting in minimal pile-soil differential settlement that could trigger downward shear stresses. Besides, stiffness differences within a group can also arise from the addition of underpinning piles to facilitate foundation reuse during vertical building expansions, a strategy increasingly adopted to meet soaring urban housing demands [50]. In short, the use of dissimilar pile lengths inherently introduces stiffness gradation, which helps to redistribute stresses more evenly between piles and soil while reducing differential settlement and improving load-sharing efficiency.

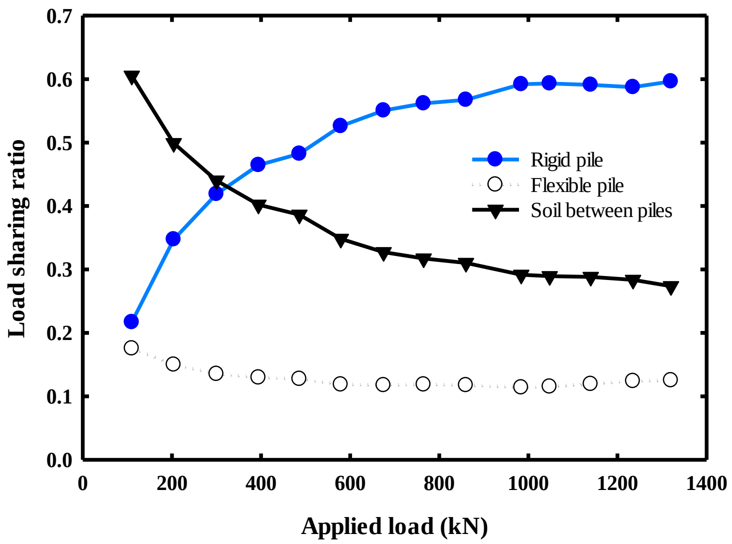

Figure 5. The load sharing ratio variation of rigid pile, flexible pile and soil between piles during vertical loading on disconnected piled rafts [49]

2.4. Dissimilarity in Configuration

Beyond the properties of individual piles, the spatial arrangement, or dissimilarity in configuration, governs how these variably-stiff elements interact as a unified system. Optimizing the layout is vital to harnessing the benefits of length, diameter, and stiffness variations for improved group performance. Conventional pile group design typically uses identical piles in a regular grid to simplify construction and minimize installation errors. The configuration of piles within a group, including their geometry, length, and layout, directly governs the foundation's load distribution and stress mechanisms, thereby critically influencing the overall structural performance and seismic resilience. In actual engineering practice, the two most common and fundamental configurations are the triangular pattern and the square layout [51]. The first arrangement is characterized by equal spacing in both perpendicular directions, and is widely used due to its straightforward design and ease of construction. On the other hand, the triangular arrangement spaces the piles at equal distances from each other, forming a series of equilateral triangles. This pattern offers the most compact grouping for a given pile spacing, minimizing the area of the raft and often leading to a higher group efficiency due to more optimal pile-to-pile interaction and better utilization of the inter-pile soil. Nonetheless, irrespective of whether a square or triangular pattern is employed, optimizing a pile group through variable pile lengths provides a more straightforward approach. This method avoids the increased positioning complexity inherent in variable pile spacing and the construction difficulties associated with installing piles of differing diameters [52].

Maheetharan et al. [53] found that using a non-uniform pile configuration, which had longer piles under the core and shorter piles along the raft perimeter, significantly reduced differential settlement and improved the structural performance of a piled raft foundation. This practical design approach was validated through an iterative geotechnical-structural modelling process and field measurements on a high-rise project. The numerical study by Zhang et al. [4] strongly supports this concept, demonstrating through finite element analysis that varying pile lengths or diameters across a group minimizes differential settlement by counteracting the inherent basin-shaped deformation pattern caused by pile-to-pile interaction effects. This shows that pile arrangements that stagger more piles at the center of a raft foundation have been shown to significantly enhance load-settlement behavior by improving the stiffness distribution and reducing differential settlements. Therefore, concentrating piles centrally to create a stiffer zone (either through non-uniform pile arrangements by increasing number, diameter, or length) effectively reduces differential settlements and improves load transfer by optimizing group interaction.

3. Modelling Interactive Effects in Dissimilar Pile Groups

3.1. Analytical Framework for Dissimilar Pile Groups

In the classical interactive effects of two piles, the interaction factor analysis method assumes that identical piles affect each other equally. It ignores the effect of dissimilarity in the group, in which, for instance, the influence of a long pile on a short pile may be greater than the reverse. This method, first formalized by Poulos [54], has long served as a cornerstone in the analysis of pile group behavior, which is often rooted in the elastic superposition of two-pile interaction factors. Several studies have been conducted to account for several missing factors in the traditional pile-pile interaction factor α_{ef} between the loaded pile *f* and unloaded equal length pile *e*, as shown in Figure 6-a. With the central concepts of pile 'sheltering' and 'reinforcing' effects, Wang et al. [55] proposed a formulation based on the logarithmic soil displacement attenuation function developed by Mylonakis & Gazetas [56] and compared it with the case presented by Poulos & Davis [57], as shown in Figure 6-b. In Figure 6-b, the subscript 1 and 2 stand for loaded 'source' pile and unloaded 'receiver' pile, respectively; as in W_{11} = settlement of 'source' pile 1, W_{21} = additional settlement of 'receiver' pile 2 caused by 'source' pile 1. Whereas the free-field displacement surrounding the loaded 'source' pile is denoted by ψ_{21}, while the 'sheltering effect' and 'reinforcing effect' are represented by $\Delta\alpha_{21}$ and $\Delta\alpha_{12}$', respectively.

Their method can be employed to analyze the sheltering and reinforcing effect of the group to estimate the load settlement response of individual piles, such as the corner, edge and center piles. However, as critically examined by Sales & Curado [58], these methods inherently assume homogeneity, reciprocity, and isolation. They argued that these presumptions dissolve in real-world conditions. Their work demonstrates that interaction factors (α) are not reciprocal ($\alpha_{ij} \neq \alpha_{ji}$) and are profoundly influenced by the stiffness of neighboring piles, the shielding effect of intermediate piles, and the geometric confinement within the group. For varying pile lengths, the interaction factors for the cases in Figure 6-a (*ii* and *iii*) can be deduced based on the identical piles' interaction coefficients α_{ee} and α_{ff}, respectively [59]. This indicates that, for a foundation utilizing varying length piles, where end-bearing and floating piles coexist, the simplifications made in the traditional approach can lead to a severe miscalculation of differential settlements and load distribution, potentially compromising the serviceability and integrity of the entire superstructure.

Advancing beyond these conventional elastic approaches, several researchers have put efforts into the development of sophisticated nonlinear 3D analytical methods to more accurately capture the complex soil-structure interaction inherent in piled raft systems [20, 21]. These interactions include soil surface-soil surface, pile-soil surface, pile-pile, raft-pile, raft-soil surface, including raft-cushion, and cushion-pile-soil-interactions in the case of disconnected piled raft [7, 60]. For convenience, Jeong & Cho [20], and Jeong et al. [61] developed an improved analytical method that incorporates raft flexibility via flat-shell elements and soil nonlinearity through load-transfer curves (*p-y*, *t-z*, *q-z*), providing a more realistic computational framework for predicting piled raft behavior. Mu et al. [60] developed a hybrid analytical approach that incorporates pile-soil-raft interactions via modified Vesic's subgrade modulus and layered soil modelling through shear displacement and elastic foundation beam methods. Similarly, El-Garhy [62] established a simplified nonlinear method based on a plate‐on‐springs approach that idealizes the cushion as an incompressible shear layer and represents the weak soil, short piles, and long piles as interacting soft, semi‐stiff, and stiff nonlinear springs to analyze disconnected piled raft foundations with piles of varying lengths and cushion‐mediated load transfer. Furthermore, moving beyond the foundation itself, Ko et al. [21] emphasized the critical need to integrate the superstructure into the analysis, proposing an iterative and interactive design method that couples the stiffness of the superstructure, the piled raft, and the soil. This body of work represents a significant shift from isolated, elastic two-pile analysis towards integrated, nonlinear 3D methods that can faithfully simulate the complex dialogue between all components of a piled raft foundation system.

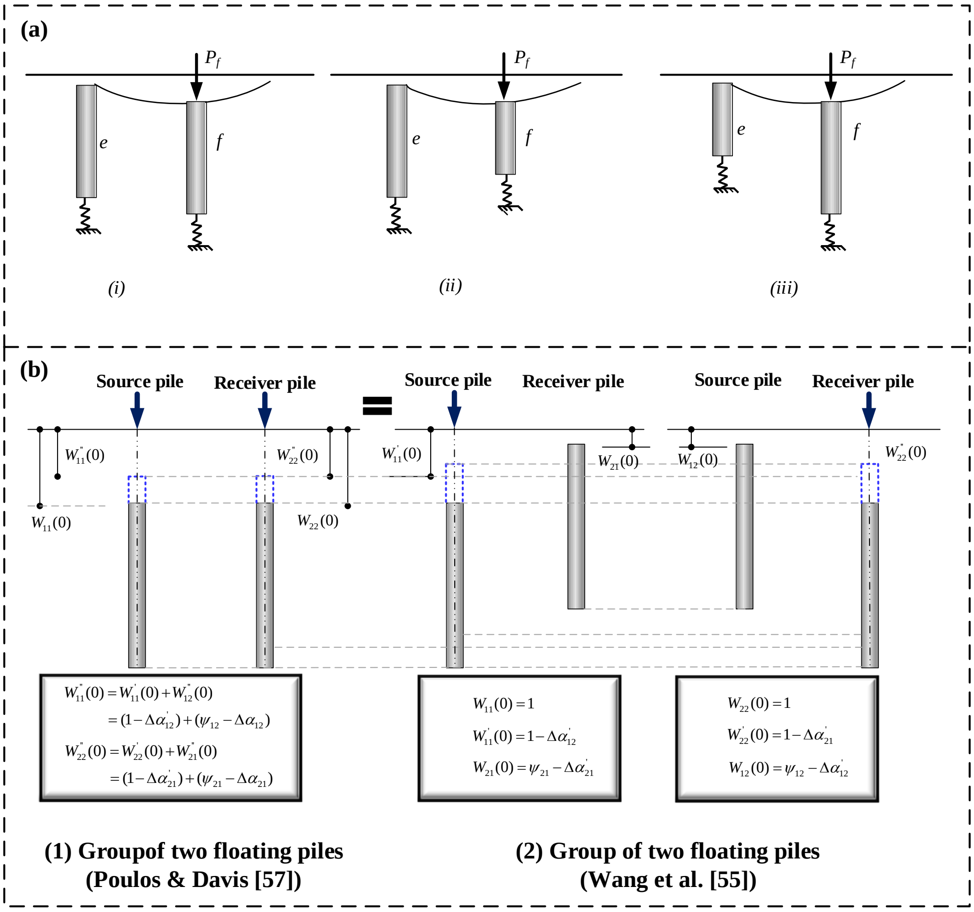

Figure 6. The pile interaction between two dissimilar piles: (a - *i*) $L_f = L_e$; (a- *ii*) $L_f < L_e$ and (a- *iii*) $L_f > L_e$; (b) two-pile interaction factor model for identical piles (*1*) the original approach according to Poulos and Davis [57], and (*2*) modified by Wang et al. [55] to consider group reinforcing/sheltering effects.

3.2. Incorporating the Cushion Effect

Referring to Figure 7-a, a typical disconnected piled raft having varying length piles can possibly involve raft-cushion, pile-cushion, long-short pile, pile-soil-pile, and cushion-soil interactions. The most common simplified representation of these interactions is the use of the plate (membrane) on springs approach, which refines the traditional Winkler model to incorporate the shear transfer between adjacent springs [61, 62]. As the load acting on the raft is transferred from the raft to the cushion (Figure 7-b), the raft is modeled as a plate pushing down the cushion springs. Due to its mechanical properties, the granular cushion is not just a set of independent vertical springs. Therefore, it is prudent to idealize it as an incompressible shear layer that allows the redistribution of loads horizontally from areas of high deflection (e.g., soil between piles) to areas of low deflection directly above the pile heads. This pressure distribution over the deflection zones transfers down to the grid of interactive springs, springs representing the soil and piles as illustrated in Figure 7-c. The stiffness of each spring element determines how much load it attracts. As shown in Figure 7-d, the long piles, being the stiffest, attract the most load (say $N_{0,j}$), but the cushion ensures that the weaker soil (with σ_{s0}) and short piles (with $N_{0,i}$) also participate significantly. These transmitted loads are then transferred to the ground using a system of interconnected springs to represent the soil-pile continuum. The cushion layer is the critical enabler in creating the condition that promotes greater settlement of the shallow soil relative to the piles in the upper section near to the pile heads. This interactive mechanism inevitably causes soil downdrag along the pile length above the neutral plane, triggering the mobilization of negative shaft friction.

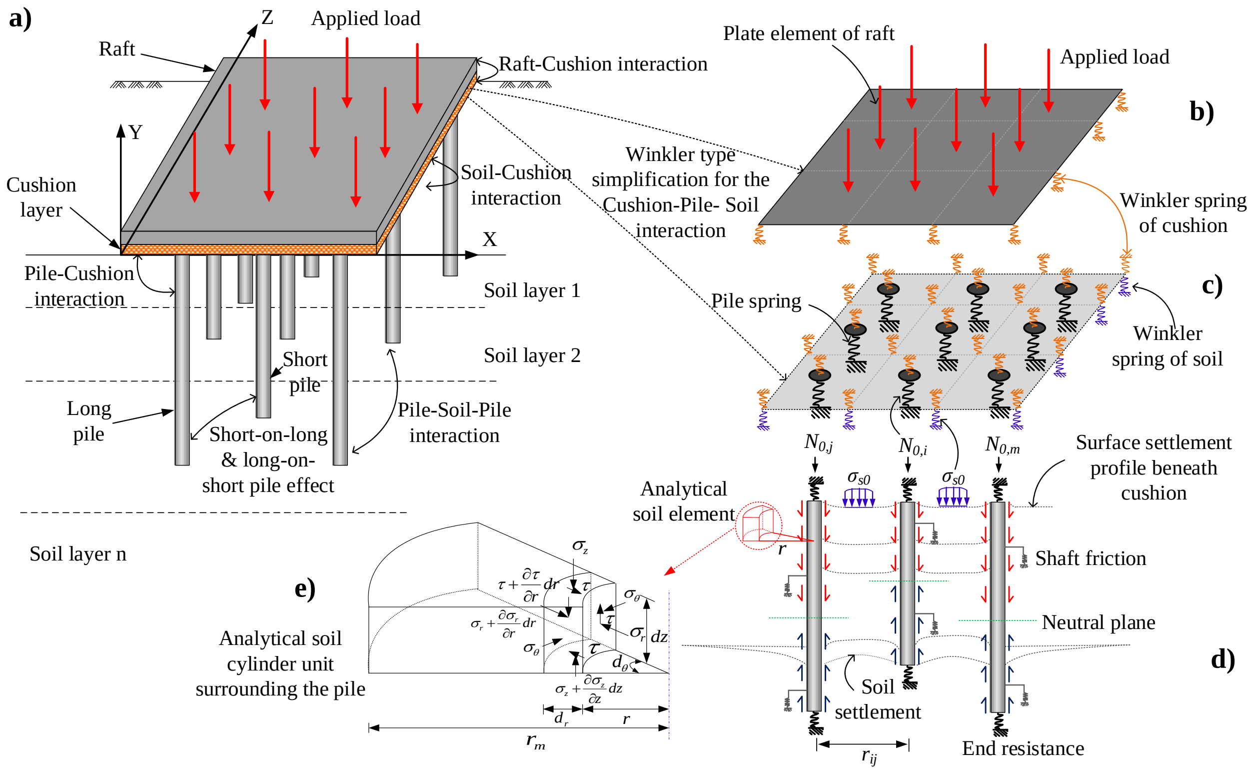

Figure 7. Simplified illustrative model for interactions and soil stress states around piles in disconnected piled raft foundations (modified after [1, 20, 63, 64])

Figures 7-a and 7-d also illustrate that the interaction for variable-length piles in a group includes both shaft and base effects [4]. This highlights a critical difference from uniformly long piles, where interactions are often simplified or considered independently. In long-short pile configurations, the longer pile's deeper base resistance influences the soil zone around the shorter pile's shaft and base, while the shorter pile's shaft resistance affects the settlement and load response of the longer pile. These coupled shaft-base interactions mean that the load-settlement behavior cannot be accurately captured by considering shaft or base effects in isolation, necessitating advanced analytical methods that account for this combined mechanism to predict group settlement and load distribution reliably.

As far back as the late 1970s, the representation of the stresses on soil elements neighboring a pile shown in Figure 7-e has been considered to analyze the diffusion of stresses from vertically loaded piles [65]. This representation allows for the theoretical foundation to develop and solve the governing equations for the stress and displacement compatibility as the infinitesimal pile and soil elements maintain equilibrium against the transmitted shear displacement in the soil induced by relative soil-pile displacement. This formulation gave rise to the classical shear displacement method, establishing the basis for mechanistic *t-z* curve derivation [66]. To date, numerous studies have extended the shear displacement method using load-transfer functions to model the progressive deformation of the pile-soil system [24, 27, 67–69]. The most commonly used load transfer functions in the load transfer method are the piecewise-hyperbolic, power-law, bilinear or trilinear relationships [70–79].

According to Liu et al. [24], the hyperbolic load transfer function (akin to Figure 8) can be used to model the interaction between dissimilar piles in a group. Each pile is first discretized into n segments of equal thickness Δz before applying the equilibrium and compatibility equations. The hyperbolic models for the shaft and base resistance mobilization can be expressed as:

$$\tau_i(z) = \frac{w_{i,rel}(z)}{a + b w_{i,rel}(z)} = \frac{w_{i,rel}(z)}{\frac{r_0}{G_s} \ln\left(\frac{r_m}{r_0}\right) + \frac{R_{sf}}{\tau_{su}} w_{i,rel}(z)} \tag{1}$$

where $w_{i,rel}(z)$ = the relative pile -soil displacement, a, b = model parameters, R_{sf}= a curve-shape constant, ranging between 0.80 and 0.95 [27], $\tau_{su}(z) = c_a + K_0(\gamma z + \sigma_{s0}) \tan\phi$, γ= soil unit weight, c_a= cohesion, and $\emptyset$ = interface friction angle.

$$\tau_b = \frac{w_b}{A + B w_b} = \frac{w_b}{\frac{\pi r_0 (1-\nu_b)}{4 G_s} + \frac{R_{bf}}{\tau_{bu}} w_b} \tag{2}$$

where A, B= spring stiffness parameters, w_b = pile toe settlement, τ_b = unit toe resistance, R_{bf} = curve-fitting coefficient, recommended to take it as 0.9 [68] and τ_{bu} = maximum unit toe resistance under the highest load.

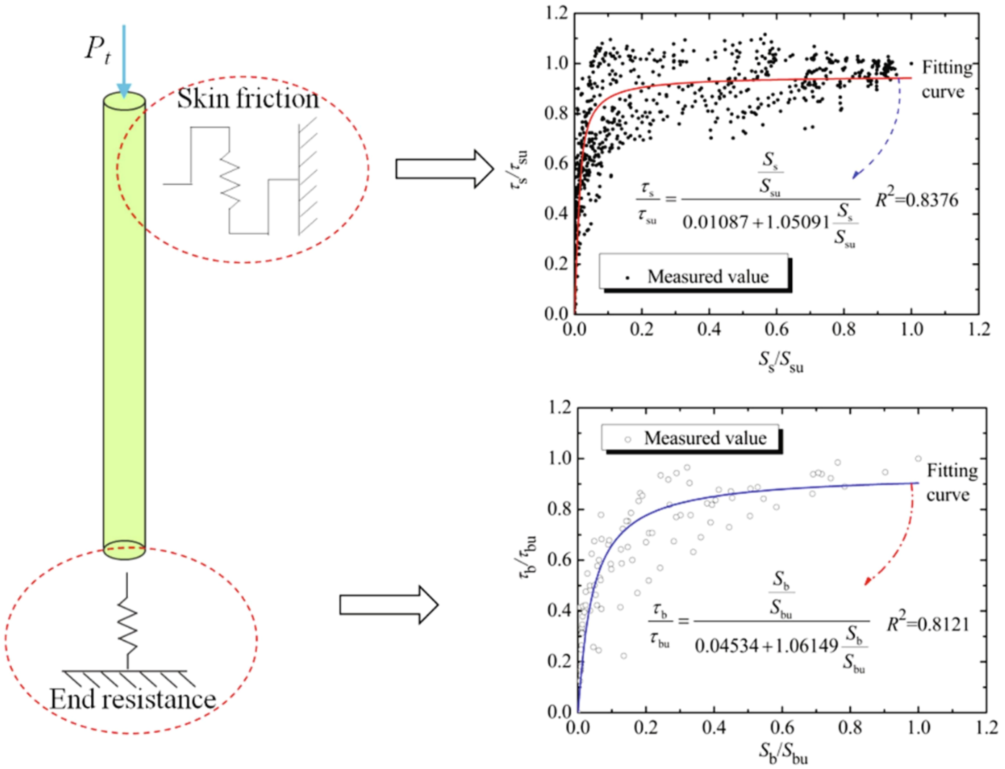

Figure 8. Typical parabolic expressions of the load transfer functions (adopted from Liu et al. [24] with permission)

Following Liu et al. [24], group interaction can be accounted for in the initial tangents of the t-z and q-z load transfer laws of Equations 1 and 2. For uniform pile-group interaction, in addition to the additional soil deformation at pile *i* due to each adjacent pile $j \neq i$, there is a reduction (or screening) that accounts for the loaded pile being "stiffened" by its neighbors, which can be expressed with the equivalent interface stiffnesses as follows:

$$a_i = \frac{1}{K_{si}} = \underbrace{\frac{r_0}{G_s} ln\frac{r_m}{r_0}}_{\text{Individual initial stiffness contribution}} + \underbrace{\sum_{j\neq i}\frac{r_0}{G_s} ln\frac{r_m}{r_{ij}}}_{\text{Neighbor-induced contribution}} - \underbrace{\sum_{j=1,j\neq i}\frac{r_0}{G_s} ln\frac{r_m}{r_{ij}}}_{\text{Screening}} \quad (3)$$

$$A_{b,i} = \frac{1}{K_{b,i}} = \frac{r_0(1-v_b)}{G_b}\left(\frac{\pi}{4}+\frac{r_0}{2}\sum_{j=1,j\neq i}\frac{1}{r_0}\right) \quad (4)$$

For dissimilar piles, however, shaft-shaft and shaft-base influences can be explicitly coupled with the same concept as follows [24]:

$$K_{si} = \frac{1}{a_i} = \left[\frac{r_0}{G_s} ln\frac{r_m}{r_0} + \sum_{j\neq i}\frac{r_0}{G_s} ln\frac{r_m}{r_{ij}} + \ldots\right]^{-1} \quad (5)$$

$$K_{b,i} = \frac{1}{A_{b,i}} = \frac{2G_b}{{r_0}^2(1-v_b)}\sum_{j\neq i}\frac{1}{r_{ij}} \quad (6)$$

Equations 3 and 4 show that equivalent shaft stiffness combines self-loading, neighbor shaft resistance, and reduction terms, in which extra terms appear to capture the cross-effects of long pile shafts, short pile shafts, and even the short pile base. Moreover, when long and short piles coexist, the formulation assumes that long pile base stiffness is affected only by other long pile toes, ignoring short pile base influence. Whereas, the short pile base stiffness accounts for both short-pile and long-pile toe interactions. The reason for this asymmetric assumption is that the short pile toe is at a higher elevation and does not significantly influence long pile tip settlement.

For the cushion-pile-soil interaction using the Winkler-type model, the displacement compatibility at the rigid raft base for the unit cell analytical element above the pile head (see Figure 8) can be expressed as follows for the internal soil column and external soil cylinder [80–82]:

$$\begin{cases} w_R - u_{p,i} = \frac{N_{0,i} t_c}{E_c A_p} \\ w_R - s_{0,i} = \frac{\sigma_{s0} t_c}{E_c} \end{cases} \quad (7)$$

where, w_R= the raft settlement, $u_{p,i}$= the pile head puncture into the cushion, $N_{0,i}$= the pile head load, t_c= thickness of the cushion, E_c= Young's modulus of the cushion, A_p= cross-sectional area of the pile, $S_{0,i}$= the surface settlement of the soil between the piles, and σ_{s0}= the stress transferred to the surface of the soil between the piles. This should satisfy the total equilibrium:

$$\sum_{i=1}^{n} N_{0,i} + \sigma_{s0} \times A_s = Q_R \tag{8}$$

where, A_s= the area of soil beneath the raft, Q_R= the total applied load on the raft supported by reinforced soil.

Based on Figure 9, the following key relationships describing the load transmission and settlement behavior of the cushion-pile-soil system can be derived [19, 81, 83]:

$$\begin{cases} w_s = S_{s1} - S_{s2} \\ w_p = S_{p1} - S_{p2} \\ S_{s1} = S_{p1} - \delta_{up} \\ S_{s2} = S_{p2} - \delta_{down} \end{cases} \tag{9}$$

$$A = B_r \times L_r = A_p + A_s \Rightarrow m = \frac{A_p}{A_s} \tag{10}$$

$$n_t = \frac{\alpha_p}{m(1-\alpha_p)} \tag{11}$$

$$\sigma_{p0} = \frac{m n_t Q_R}{(m+1)(n_t m - m + 1)} \tag{12}$$

$$\sigma_{s0} = \frac{m Q_R}{(m+1)(n_t m - m + 1)} \tag{13}$$

$$\delta_{up} = \frac{(1-{\mu_1}^2)\times\sqrt{A_p}}{E_1}(\sigma_{p0} - \sigma_{s0}) \tag{14}$$

$$\delta_{down} = \frac{(1-{\mu_2}^2)\times\sqrt{A_p}}{E_2}(\sigma_{pb} - \sigma_{sb}) \tag{15}$$

where; $w_s = w_p + \delta_{up} + \delta_{down}$= total deformation of soil around the pile, w_p = the compression of the pile, S_{s1}, S_{s2} = soil deformations of at the pile head and toe surface levels, respectively; S_{p1}, S_{p2} = pile's top and toe settlements, respectively; and δ_{up}, δ_{down} = pile's head and toe penetrations, respectively; A, B_r, L_r = area, breadth and length of the raft, respectively, A_p = pile's cross-sectional area of single pile, A_s = soil's area, m = the ratio of the surface per reinforcing element cross-sectional area, n_t = the ratio of pressure at pile head (σ_{p0}) to that taken by the soil (σ_{s0}), α_p = the pile load sharing ratio, representing the portion of total load directed to the pile in reference to the applied total force, E_1 and E_2= the elastic modulus of cushion and underlying soil stratum, respectively, χ = the empirical coefficient of settlement calculation, which can be taken as 0.79 for circular loading surface and 0.88 for square loading surface [84], σ_{pb} = pile base stress, and σ_{sb} =the surrounding soil bottom stress.

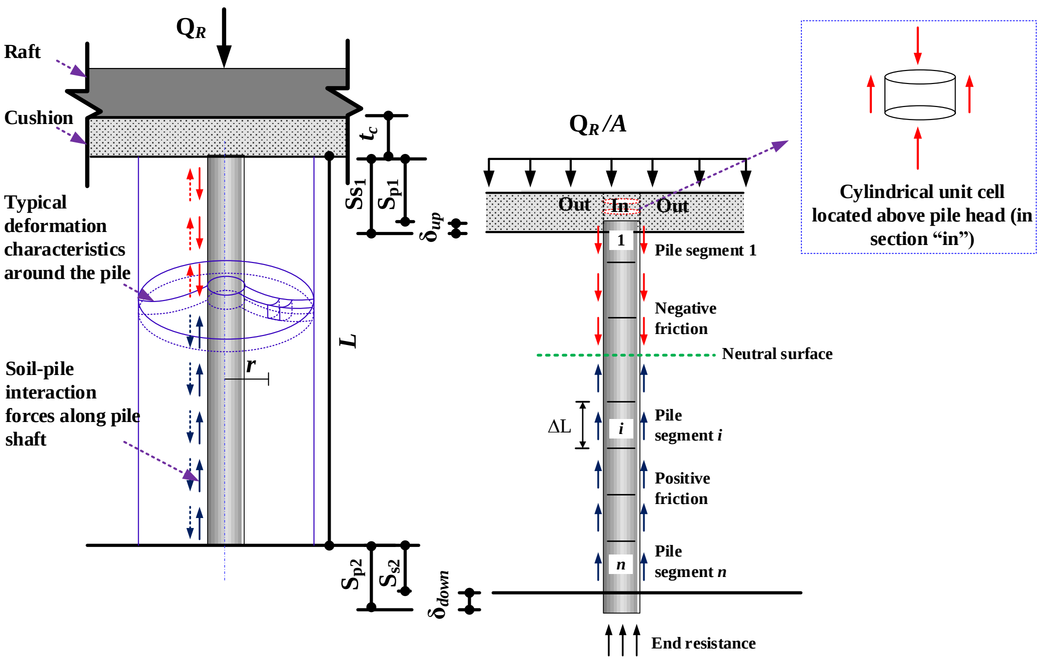

Figure 9. Schematic representation of the cushion-pile-soil interaction [19, 81, 83]

Now, with the above expressions, the disconnected piled raft foundation's basic load-displacement relationship is as follows for the joint action of the long piles, short piles, soil, and cushion system:

$$[K]\{w\} = \{Q_R\} \tag{16}$$

where, [K] is global stiffness matrix of the soil-pile-cushion system, $\{w\}$ and $\{Q_R\}$are the vertical displacement vectors and applied load vectors of the corresponding nodes, respectively.

In this formulation, each pile head interacts with the raft through a nonlinear cushion. As the applied load increases, the cushion redistributes pressure laterally from high-deflection zones to low-deflection zones before the load enters the soil and pile springs by following the "plate (membrane) on springs" concept as mentioned previously. For each pile *i*, pile-cushion compatibility at the head enforces equality of pile axial force and cushion reaction, while the compression of the cushion over the piles head creates a relative pile-soil displacement. The larger near-pile head soil displacement produces a downward pressure on the pile shaft, generating negative skin friction that migrates down to the neutral plane. This phenomenon can be reflected using the relative pile-soil displacement in Equation 17, where z_n is the depth at which the neutral plane satisfies $w_{i_{,rel}}(z_n) = 0$and the reversal from negative to positive shaft friction occurs.

$$\begin{cases} w_{i_{,rel}}(z) < 0, \text{where } w_{p,i}(z) < w_{s,i}(z) \Rightarrow \tau_i(z) < 0, (0 \le z < z_n) \\ w_{i_{,rel}}(z_n) = 0 \Rightarrow \text{ neutral plane} \\ w_{i_{,rel}}(z) > 0, \text{where } w_{p,i}(z) > w_{s,i}(z) \Rightarrow \tau_i(z) > 0, (z_n < z) \end{cases} \tag{17}$$

where $w_{p,i}(z)$ and $w_{s,i}(z)$ denote the vertical displacements of the pile and of the surrounding soil at depth z, respectively.

Considering that the pile and the surrounding soil undergo the same settlement at the neutral plane depth, the corresponding deformation-compatibility relations for the regions above and below this plane can be expressed as:

$$\begin{cases} w_{su} = w_{pu} + \delta_{up} \\ w_{sd} = w_{pd} + \delta_{down} \end{cases} \tag{17}$$

where $w_{su}$and w_{pu}denote the compressive deformations of the soil between piles and the rigid pile above the neutral plane, respectively; $w_{sd}$and w_{pd} denote the corresponding deformations below the neutral plane.

The pile displacement overtakes the soil displacement progressively from the neutral plane downward so the zone of positive skin friction expands with load. In order to capture this, the pile-soil interaction is represented by hyperbolic t-z and q-z relations (Equations 1 and 2), while group effects enter through the tangents obtained from the equivalent-stiffness expressions of Equations 5 and 6. Finally, the piled raft response follows from the head compatibility (Equations 7 and 8) and overall equilibrium (Equation 16).

For convenience, the pile base penetration, S_b, which is the last segment's settlement, can be corrected by the deformation attributed to the pile toe stress and the bottom stress calculated on the surrounding soil using Equation 15, $S_{b'}$. If there is disagreement between the computed pile base penetration, adjustment of the α_p is to be made for another iterative back analysis. Figure 2-b presents the flowchart for the solution procedure.

3.3. Validation of Analysis

3.3.1. Pile group Composed of Unequal-length Piles

Figure 10 shows the back calculation results of the experimental findings on a 2×2 long and short pile disconnected piled raft foundation reported by Guo et al. [28]. The indoor model test setup involved a large-scale model box of dimensions 1600 mm × 1600 mm × 2500 mm, instrumented piles made from hollow aluminium tubes of external diameter 100 mm with knurled surfaces to enhance soil-pile friction, a medium river sand as the analogous subsoil, and a cushion layer. The instrumentation included strain gauges attached to the piles, earth pressure cells, and pressure sensors to monitor load transfer and stress distribution. As can be shown, the comparison of the computation resulted in relatively close pile load sharing ratios.

Initially, the subsoil carries a significant portion of the load. This is because the cushion layer first makes contact with the larger surface area of the soil between the piles, and the pile-soil interfaces are not yet fully mobilized. As settlement progresses, the hyperbolic load-transfer functions (Equations 1 and 2) govern the progressive mobilization of shaft and base resistance. The long piles, due to their greater embedded length, develop a significantly higher composite stiffness by engaging a larger shaft area and deriving end-bearing from deeper, stiffer soil strata. Consequently, they attract an increasing and disproportionately larger share of the load, as the load naturally seeks the stiffer load path. The shorter piles stay comparatively under-mobilized because their shaft length is limited for more mobilizable interface area. Although the pile-soil synergistic mechanical behavior can be captured well, the computation using the proposed method yielded conservative results, probably as a consequence of simplifying the cushion as a Winkler-type spring layer. The calculation may slightly oversimplify the complex shear transfer and arching effects within a real cushion layer.

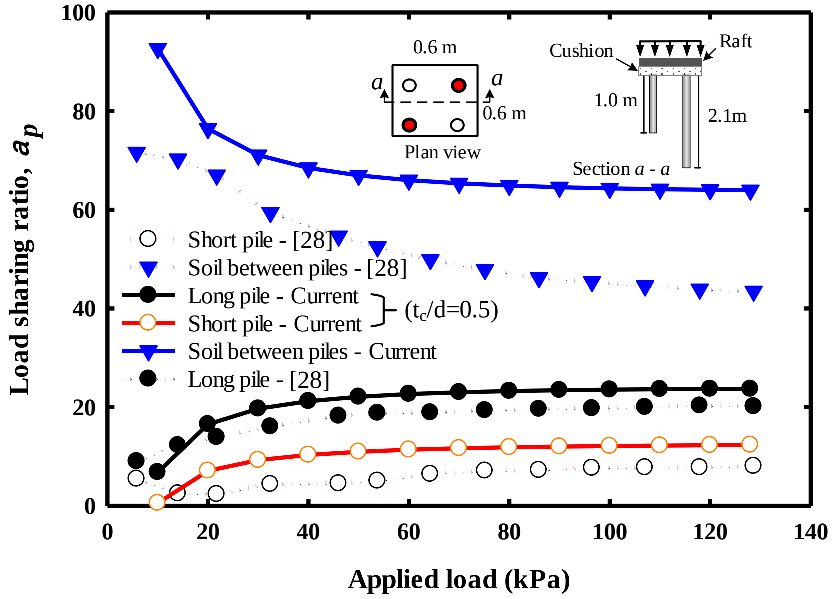

Figure 10. Comparison of computational results with the load sharing ratio variation from experimental results on variable length piles [28]

3.3.2. Pile Group Composed of Variable Pile Diameters

Liu et al [13] conducted experimental and theoretical study to investigate the response of disconnected piled raft composite foundation with variable pile diameters. The experimental setup consisted of a large-scale indoor model tank of dimensions 2000mm×2000mm×4000mm, four hollow aluminium piles embedded in silty sand, each 2 m long, with surface knurling to simulate the roughness of real concrete piles and ensure realistic pile-soil interface friction. A 50 mm-thick medium coarse sand cushion layer was placed above the piles under a steel load plate subjected to a uniformly distributed load. From the three test groups with different diameter combinations, the configuration with pile dimeters of 80 mm and 120 mm, arranged in a square pattern with a center-to-center spacing of 320 mm, is back calculated. The comparison between computed load sharing ratio and the results from Liu et al.'s experimental setup is shown in Figure 11.

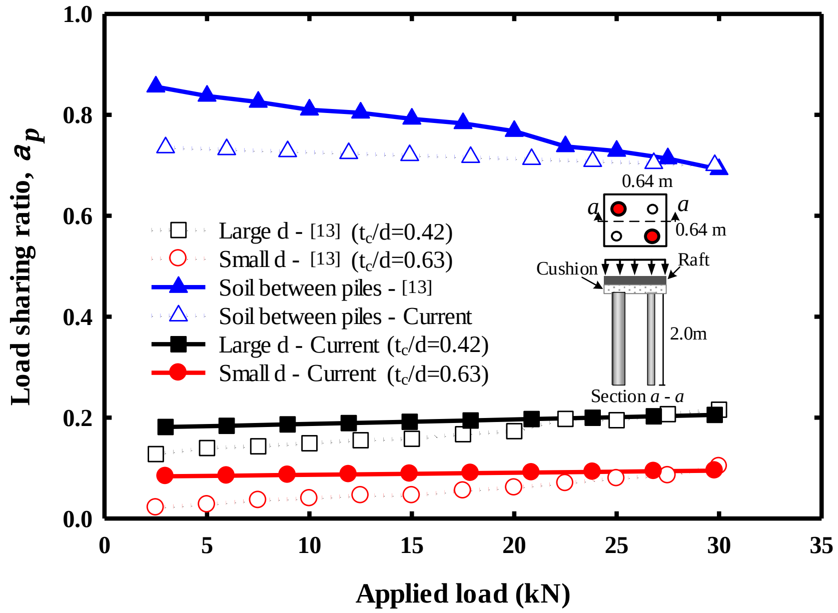

Figure 11. Comparison of computational results with the load sharing ratio variation from experimental results on variable diameter piles [13]

Unlike the variable-length case, where stiffness differences develop with depth, dissimilarity in diameter creates an immediate and stark contrast in pile head stiffness. It holds that, larger-diameter piles possess a greater cross-sectional area (resulting in higher axial rigidity), and a larger shaft perimeter, leading to a higher initial equivalent stiffness ($K_{s,i}$, $K_{b,i}$) from the outset of loading. Consequently, the larger-diameter piles attract a much greater load share even at low load levels. In addition, the cushion effectively facilitates the interaction by ensuring that the smaller-diameter piles and subsoil continue to participate significantly. However, as the load-sharing ratio for stiffer elements increases as the applied load increases, the subsoil fraction decreases. The close agreement between computation and experiment in Figure 11 provides high confidence in using the proposed analytical framework for optimizing group configurations where varying pile diameters are used to balance load distribution and material efficiency under a raft.

4. Conclusions

This article gives insights into the load-carrying and interactive mechanism of a piled raft foundation having dissimilar piles by implementing both the shaft-friction and end-bearing laws in hyperbolic form and with the interaction rules for dissimilar piles set out by Liu et al. [24]. The following can be summarized:

- The interactive effects of pile dissimilarity significantly influence the load sharing ratio of disconnected piled raft foundations. For rafts resting on dissimilar piles, longer (or larger diameter) piles attract a disproportionately higher share of the applied load compared to shorter (or smaller diameter) piles. This is because stiffer components in a load-sharing system attract a greater share of the load. The stiffness of a pile-soil unit is not just the stiffness of the pile material itself but the composite stiffness of the pile and the surrounding soil working together. Accordingly, a longer pile is a stiffer pile-soil unit. Moreover, the larger cross-sectional area and higher bending stiffness of big-diameter piles make them stiffer elements. The use of dissimilar piles inherently introduces stiffness gradation that affects the pile-soil synergistic mechanism.
- In a group of dissimilar piles, the presence of multiple piles reduces the individual pile stiffness due to overlapping stress zones and reduced soil confinement. This exacerbates the asymmetric nature of pile-to-pile interactions. In order to overcome the mathematical difficulty of having two dissimilar piles in different locations, superposition of stiffness modifiers can be employed with the concept of Equivalent Stiffness of the Pile-Soil Interface. This simplified approach predicts the interactive effects such that center piles, which are surrounded by other piles, will have the softest equivalent stiffness and thus the largest settlement. This allows for the optimization of pile groups by showing that using longer (or larger-diameter) piles in the center and shorter (or smaller) ones at the edges can effectively reduce differential settlement.
- With the adaptation of the equivalent stiffness of dissimilar pile types and the hyperbolic load transfer function, the cushion-pile-soil interaction at the pile heads was introduced into the load sharing ratio analysis. Since crowning the piles with an intercalated cushion layer further complicates the pile load-transfer computation, the cushion layer is simplified by the Winkler-type spring. The results were compared with existing data on rafts resting on cushioned variable-length and -diameter piles. The comparison shows relatively conservative results at low load intensity but comparable output when the applied load increases. The procedure used in the current study can be adopted for preliminary design to assess dissimilar pile group optimization.
- Although the insights from the current study greatly improve the current understanding of disconnected piled raft foundations with dissimilar piles, the approach is limited by simplifying the cushion through springs and ignoring the influence of a long pile's base resistance on the shaft stiffness of a short pile. These assumptions reduce complexity while retaining the most significant interactive effects under vertical static loading conditions and do not encompass the effects of soil stiffness degradation under cyclic or long-term repeated loads. Moreover, as performance-based design becomes the norm, there is a growing need for adaptive modelling frameworks that can simulate the nonlinear, coupled behavior of mixed-length piles under various loading scenarios. Further research is required to verify the results through full-scale field monitoring and machine learning-driven predictive analytics.

5. Declarations

5.1. Author Contributions

Conceptualization, B.U.U., Y.G., and Z.J.; methodology, Y.L.; software, Y.G.; validation, M.M. and C.L.; formal analysis, B.U.U. and Y.X.; writing—original draft preparation, B.U.U.; writing—review and editing, Y.L., M.M., and C.L.; visualization, B.U.U. and Y.X.; supervision and project administration, Y.G. and Z.J.; funding acquisition, Y.G. and Y.L. All authors have read and agreed to the published version of the manuscript.

5.2. Data Availability Statement

The data presented in this study are available in article.

5.3. Funding and Acknowledgments

The authors acknowledge the research funding and financial support from the Henan Provincial Key R&D Project, Safety Key Technology and Application Demonstration of Urban Underground Space Construction (Grant No. 231111322100) and Henan Province Science and Technology Key Project (Grant No. 252102240027 and Grant No. 242102320006).

5.4. Conflicts of Interest

The authors declare no conflict of interest.

6. References

[1] Taghavi Ghalesari, A., & Janalizadeh Choobbasti, A. (2018). Numerical analysis of settlement and bearing behaviour of piled raft in Babol clay. European Journal of Environmental and Civil Engineering, 22(8), 978-1003. doi:10.1080/19648189.2016.1229230.

[2] Poulos, H. G. (2016). Tall building foundations: design methods and applications. Innovative Infrastructure Solutions, 1(1), 10. doi:10.1007/s41062-016-0010-2.

[3] Leung, Y. F., Klar, A., & Soga, K. (2010). Theoretical Study on Pile Length Optimization of Pile Groups and Piled Rafts. Journal of Geotechnical and Geoenvironmental Engineering, 136(2), 319–330. doi:10.1061/(asce)gt.1943-5606.0000206.

[4] Zhang, Q. Q., Liu, S. W., Feng, R. F., Qian, J. G., & Cui, C. Y. (2020). Finite element prediction on the response of non-uniformly arranged pile groups considering progressive failure of pile-soil system. Frontiers of Structural and Civil Engineering, 14(4), 961–982. doi:10.1007/s11709-020-0632-5.

[5] Burland, J. B., Broms, B. B., & De Mello, V. F. (1978). Behaviour of foundations and structures. Proceeding of 9th International Conference on Soil Mechanics and Foundation Engineering, 10-15 July, 1977, Tokyo, Japan.

[6] Fioravante, V. (2011). Load transfer from a raft to a pile with an interposed layer. Geotechnique, 61(2), 121–132. doi:10.1680/geot.7.00187.

[7] Guo, Y., Liu, Y., Wei, Y., Zhao, J., & Uge, B. U. (2023). Load-Settlement Response of Cushioned Piled Rafts with Varying Pile Lengths to Retaining Wall Movement. Geotechnical and Geological Engineering, 41(5), 3093–3113. doi:10.1007/s10706-023-02446-0.

[8] Mu, L., Chen, W., Huang, M., & Lu, Q. (2020). Hybrid Method for Predicting the Response of a Pile-Raft Foundation to Adjacent Braced Excavation. International Journal of Geomechanics, 20(4). doi:10.1061/(asce)gm.1943-5622.0001627.

[9] Uge, B. U., Guo, Y., Zhao, J., Liu, Y., Shumuye, E. D., Mehmood, M., & Tekle, M. H. (2025). A review of the load-carrying mechanism of connected and disconnected piled-raft foundations under static and dynamic loading. Sādhanā, 50(4), 1-31. doi:10.1007/s12046-025-02837-4.

[10] Wu, T., Sun, Z., Tan, W., Kasu, C. M., & Gong, J. (2022). Response of vertically-loaded pile in spatially-variable cement-treated soil. PLOS ONE, 17(4), e0266975. doi:10.1371/journal.pone.0266975.

[11] Zhang, Y., Huang, J., Xie, J., Jiang, S. H., & Zeng, C. (2025). Deep learning-based calibration of resistance factors for pile groups with load tests. Acta Geotechnica, 20(9), 4355–4367. doi:10.1007/s11440-025-02634-7.

[12] Abdrabbo, F. M., & El-Wakil, A. Z. (2015). Behavior of pile group incorporating dissimilar pile embedded into sand. Alexandria Engineering Journal, 54(2), 175–182. doi:10.1016/j.aej.2014.11.001.

[13] Liu, Y., Gu, S., Duan, S., & Hou, S. (2024). Load Settlement Response of Composite Foundation of Variable Pile Diameters. International Journal of Geomechanics, 24(9). doi:10.1061/ijgnai.gmeng-9629.

[14] Azizkandi, A. S., Aghamolaei, M., & Hasanaklou, S. H. (2020). Evaluation of dynamic response of connected and non-connected piled raft systems using shaking table tests. Soil Dynamics and Earthquake Engineering, 139, 106366. doi:10.1016/j.soildyn.2020.106366.

[15] Bagheri, M., Ranjbar Malidarreh, N., Ghaseminejad, V., & Asgari, A. (2025). Seismic resilience assessment of RC superstructures on long–short combined piled raft foundations: 3D SSI modeling with pounding effects. Structures, 81, 110176. doi:10.1016/j.istruc.2025.110176.

[16] Akbari, A., & Eslami, A. (2025). Performance of Composite Piled Raft Foundations with Long and Short Piles Under Static and Seismic Loading. Geotechnical and Geological Engineering, 43(5), 188. doi:10.1007/s10706-025-03136-9.

[17] Pengfei, L. I., Renwang, L. I. A. N. G., & Jingluo, C. A. I. (2018). Experimental evaluation of pile-soil load sharing ratio for composite foundation with long and short piles. China Sciencepaper, 13(13), 1467.

[18] Lin, C., Liu, Q., Su, Y., Yue, C., & Zeng, L. (2024). Load transfer of the disconnected pile. Acta Geotechnica, 19(8), 5673–5684. doi:10.1007/s11440-024-02285-0.

[19] Malekkhani, M. J., & Bazaz, J. B. (2021). An Analytical Model to Study the Behavior of Non-connected Piled Rafts with Granular Cushion Subjected to Vertical Load. International Journal of Civil Engineering, 19(8), 941–956. doi:10.1007/s40999-021-00611-1.

[20] Jeong, S., & Cho, J. (2014). Proposed nonlinear 3-D analytical method for piled raft foundations. Computers and Geotechnics, 59, 112–126. doi:10.1016/j.compgeo.2014.02.009.

[21] Ko, J., Cho, J., & Jeong, S. (2017). Nonlinear 3D interactive analysis of superstructure and piled raft foundation. Engineering Structures, 143, 204–218. doi:10.1016/j.engstruct.2017.04.026.

[22] Halder, P., & Manna, B. (2021). Load transfer mechanism for connected and disconnected piled raft: a comparative study. Acta Geotechnica, 17(7), 3033–3045. doi:10.1007/s11440-021-01409-0.

[23] Alhassani, A. M. J., & Aljorany, A. N. (2023). Experimental and Numerical Modeling of Connected and Disconnected Piled Raft. KSCE Journal of Civil Engineering, 27(6), 2442–2454. doi:10.1007/s12205-023-0437-x.

[24] Liu, S., Zhang, Q., Cui, C., Feng, R., & Cui, W. (2021). A simplified approach for the response of pile groups composed of dissimilar piles. Structures, 34, 4548–4559. doi:10.1016/j.istruc.2021.10.063.

[25] Guo, Y., Zhao, J., Li, M., Liu, Y., Hou, S., & Uge, B. U. (2024). Elasto-Plastic Analysis for Load-Settlement Prediction of Vertically Loaded Cushioned Piled-Rafts with Unequal Pile Lengths. Soil Mechanics and Foundation Engineering, 61(2), 120–129. doi:10.1007/s11204-024-09952-0.

[26] Dong, X., Tan, X., Lu, Z., Zhang, P., Zha, F., & Xu, L. (2024). Reliability analysis of two–pile group in spatially variable soil considering differential settlement. Ocean Engineering, 307(118182). doi:10.1016/j.oceaneng.2024.118182.

[27] Zhang, Q., Liu, S., Zhang, S., Zhang, J., & Wang, K. (2016). Simplified non-linear approaches for response of a single pile and pile groups considering progressive deformation of pile–soil system. Soils and Foundations, 56(3), 473–484. doi:10.1016/j.sandf.2016.04.013.

[28] Guo, Y., Lv, C., Hou, S., & Liu, Y. (2021). Experimental Study on the Pile-Soil Synergistic Mechanism of Composite Foundation with Rigid Long and Short Piles. Mathematical Problems in Engineering, 2021, 1–15. doi:10.1155/2021/6657116.

[29] Cao, M., & Zhou, A. (2022). Fictitious pile method for fixed-head pile groups with dissimilar piles subjected to horizontal loading. Soils and Foundations, 62(5). doi:10.1016/j.sandf.2022.101212.

[30] Nguyen, D. D. C., Kim, D. S., & Jo, S. B. (2014). Parametric study for optimal design of large piled raft foundations on sand. Computers and Geotechnics, 55, 14–26. doi:10.1016/j.compgeo.2013.07.014.

[31] Shrestha, S., Ravichandran, N., & Rahbari, P. (2018). Geotechnical Design and Design Optimization of a Pile-Raft Foundation for Tall Onshore Wind Turbines in Multilayered Clay. International Journal of Geomechanics, 18(2), 04017143. doi:10.1061/(asce)gm.1943-5622.0001061.

[32] Zheng, J.-J., Liu, Y., Pan, Y.-T., & Hu, J. (2018). Statistical Evaluation of the Load-Settlement Response of a Multicolumn Composite Foundation. International Journal of Geomechanics, 18(4), 04018015. doi:10.1061/(asce)gm.1943-5622.0001124.

[33] Zhao, M., Zhang, L., & Yang, M. (2006). Settlement calculation for long-short composite piled raft foundation. Journal of Central South University of Technology, 13(6), 749–754. doi:10.1007/s11771-006-0026-4.

[34] Hu, K., Jiang, K., Gou, X., Wei, W., Yan, L., Zhou, T., Guo, Z., & Chen, G. (2023). Dissimilar Pile Raft Foundation Behavior under Eccentric Vertical Load in Elastic Medium. Buildings, 13(12), 3040. doi:10.3390/buildings13123040.

[35] Lv, C. Y., Guo, Y. C., Li, Y. H., Hu-Yan, A. Di, & Yao, W. M. (2023). Experimental study on the horizontal bearing characteristics of long-short-pile composite foundation. Geomechanics and Engineering, 33(4), 341–352. doi:10.12989/gae.2023.33.4.341.

[36] Uge, B. U., & Guo, Y.-C. (2023). Experimental study on load sharing characteristics of long-short CFG pile composite foundation adjacent to rigid retaining wall rotating about its base. Journal of Engineering Research, 11(1), 125–135. doi:10.36909/jer.13241.

[37] Zhu, Z. R., Guan, W., Han, K., Wu, H. G., Zhao, S. Q., & Liu, X. (2023). Experimental Study on the Dynamic Characteristics of a New Long-Short Pile Composite Foundation under Long-Term Train Load. Shock and Vibration, 7032053, 1–16. doi:10.1155/2023/7032053.

[38] Bagheri, M., Jamkhaneh, M. E., & Samali, B. (2018). Effect of Seismic Soil–Pile–Structure Interaction on Mid- and High-Rise Steel Buildings Resting on a Group of Pile Foundations. International Journal of Geomechanics, 18(9), 04018103–1. doi:10.1061/(asce)gm.1943-5622.0001222.

[39] Guo, Y., Gu, S., Jin, J., & Li, M. (2021). Study on the earth pressure of a foundation pit adjacent to a composite foundation with rigid-flexible and long-short piles. PLOS ONE, 16(5), e0251985. doi:10.1371/journal.pone.0251985.

[40] Gao, F., Cheng, X., Wang, W., Lv, Q., & Cheng, X. (2024). Experimental Study on the Bearing Characteristics of Rigid-Flexible Long-Short Pile Composite Foundations in Thick Collapsible Loess Areas. KSCE Journal of Civil Engineering, 28(5), 1690–1701. doi:10.1007/s12205-024-0052-5.

[41] Zheng, J. J., Abusharar, S. W., & Wang, X. Z. (2008). Three-dimensional nonlinear finite element modeling of composite foundation formed by CFG-lime piles. Computers and Geotechnics, 35(4), 637–643. doi:10.1016/j.compgeo.2007.10.002.

[42] Tong, J. X., Sun, X. H., Luo, P. F., Jia, N., Yang, X. H., & Yan, M. L. (2014). Study on the design method of different thickness-diameter ratios for composite foundation with rigid long and short piles. Applied Mechanics and Materials, 580–583, 723–728. doi:10.4028/www.scientific.net/AMM.580-583.723.

[43] Ding, J., Wang, W., Zhao, T., Feng, J., & Zhang, P. (2013). The Dynamic Characteristic Experimental Method on the Composite Foundation with Rigid-Flexible Compound Piles. Open Journal of Civil Engineering, 3(2), 94–98. doi:10.4236/ojce.2013.32010.

[44] Liu, K., Xie, X., & Liu, H. (2010). Performance of rigid-flexible-pile foundation with cushion. Proceedings of the Institution of Civil Engineers - Geotechnical Engineering, 163(4), 221–227. doi:10.1680/geng.2010.163.4.221.

[45] Yan, F., & Huang, X. (2014). Experiment Research of Bearing Behavior on Lime-Soil Pile and CFG Pile Rigid-Flexible Pile Composite Subgrade. Proceedings of Ground Improvement and Geosynthetics, 40–48. doi:10.1061/9780784413401.004.

[46] Yang, Y., & Zhang, J. (2022). Analysis of Features of Long and Short Pile Composite Foundation in High-Rise Buildings. Soil Mechanics and Foundation Engineering, 59(1), 92–101. doi:10.1007/s11204-022-09788-6.

[47] Jais, I. B. M., Rahman, S. N. S. S. A., & Lat, D. C. (2025). 3D Numerical Analysis of Piled Raft Foundation on Soft Soil Improved by Stone Columns. Transportation Infrastructure Geotechnology, 12(1), 81. doi:10.1007/s40515-025-00539-2.

[48] Fang, X., Shen, C., Wang, C., Guo, Y., & Wang, L. (2024). Study on bearing characteristic of multi-pile composite foundation with biocemented coral sand pile. Journal of Building Engineering, 98, 111297. doi:10.1016/j.jobe.2024.111297.

[49] Zhang, E., Yu, L., & He, X. (2017). Analysis of Action Mechanism for Rigid Flexible Pile Composite Foundation. Revista Tecnica De La Facultad De Ingenieria Universidad Del Zulia, 39(11), 260–270. doi:10.21311/001.39.11.32.

[50] Oh, J.-H., Kim, S.-H., Hwang, H.-J., Chung, C.-K., & Park, H.-G. (2024). Device for Load-Redistribution between Existing Piles and Underpinning Micropiles. Journal of Geotechnical and Geoenvironmental Engineering, 150(12), 12706. doi:10.1061/jggefk.gteng-12706.

[51] Uge, B. U., & Guo, Y.-C. (2020). CFG Pile Composite Foundation: Its Engineering Applications and Research Advances. Journal of Engineering, 2020, 1–26. doi:10.1155/2020/5343472.

[52] Xie, Y., & Chi, S. (2020). Optimization Method of Reducing the Differential Settlements of Piled Raft Foundations Based on Pile-to-Pile Interaction Theory. Advances in Civil Engineering, 2020, 1–14. doi:10.1155/2020/1521876.

[53] Maheetharan, A., Raveendiraraj, A., Qusous, O., & May, R. (2016). Design of pile configuration for optimum raft performance. Proceedings of the Institution of Civil Engineers: Geotechnical Engineering, 169(2), 139–152. doi:10.1680/jgeen.15.00047.

[54] Poulos, H. G. (1989). Pile behaviour—theory and application. Géotechnique, 39(3), 365–415. doi:10.1680/geot.1989.39.3.365.

[55] Wang, A. D., Wang, W. D., Huang, M. S., & Wu, J. B. (2016). Interaction factor for large pile groups. Geotechnique Letters, 6(1), 58–65. doi:10.1680/jgele.15.00139.

[56] Mylonakis, G., & Gazetas, G. (1998). Settlement and additional internal forces of grouped piles in layered soil. Geotechnique, 48(1), 55–72. doi:10.1680/geot.1998.48.1.55.

[57] Poulos, H. G., & Davis, E. H. (1980). Pile foundation analysis and design (No. Monograph). John Wiley & Sons, Hoboken, United States.

[58] Sales, M. M., & Curado, T. da S. (2018). Interaction factor between piles: Limits on using the conventional elastic approach in pile group analysis. Soils and Rocks, 41(1), 49–60. doi:10.28927/SR.411049.

[59] Xu, J., Xu, X., & Yao, W. (2022). New calculation method for the settlement of long-short-pile composite foundation based on virtual soil-pile model. Arabian Journal of Geosciences, 15(9), 870. doi:10.1007/s12517-022-10028-2.

[60] Mu, L., Chen, Q., Huang, M., & Basack, S. (2017). Hybrid Approach for Rigid Piled-Raft Foundations Subjected to Coupled Loads in Layered Soils. International Journal of Geomechanics, 17(5), 04016122. doi:10.1061/(asce)gm.1943-5622.0000825.

[61] Jeong, S., Park, J., & Chang, D. (2024). An approximate numerical analysis of rafts and piled-rafts foundation. Computers and Geotechnics, 168, 106108. doi:10.1016/j.compgeo.2024.106108.

[62] El-Garhy, B. M. (2022). A Simplified Method for the Nonlinear Analysis of Composite Piled Raft Foundation. Geotechnical and Geological Engineering, 40(9), 4357–4375. doi:10.1007/s10706-022-02159-w.

[63] Liang, F., Chen, L., & Han, J. (2009). Integral equation method for analysis of piled rafts with dissimilar piles under vertical loading. Computers and Geotechnics, 36(3), 419–426. doi:10.1016/j.compgeo.2008.08.007.

[64] Kim, K. N., Lee, S. H., Kim, K. S., Chung, C. K., Kim, M. M., & Lee, H. S. (2001). Optimal pile arrangement for minimizing differential settlements in piled raft foundations. Computers and Geotechnics, 28(4), 235-253. doi:10.1016/S0266-352X(01)00002-7.

[65] Randolph, M. F., & Wroth, C. P. (1978). Analysis of Deformation of Vertically Loaded Piles. Journal of the Geotechnical Engineering Division, 104(12), 1465–1488. doi:10.1061/ajgeb6.0000729.

[66] Cooke, R. W. (1974). The settlement of friction pile foundations. Proceedings, Conference on Tall Buildings, 2-5 December, 1974, Kuala Lumpur, Malaysia.

[67] Liu, G., Li, J., Liu, C., & Li, P. (2025). Progressive failure analysis of axially loaded single pile embedded in unsaturated soils based on LTM coupling with SDM. Computers and Geotechnics, 179, 107036. doi:10.1016/j.compgeo.2024.107036.

[68] Zhang, Q., Liu, S., Feng, R., & Li, X. (2018). Analytical Method for Prediction of Progressive Deformation Mechanism of Existing Piles Due to Excavation Beneath a Pile-Supported Building. International Journal of Civil Engineering, 17(6), 751–763. doi:10.1007/s40999-018-0309-9.

[69] Liu, Y., & Vanapalli, S. K. (2022). Modified Shear Displacement Method for Analysis of Piles in Unsaturated Expansive Soils Considering Influence of Environmental Factors. International Journal of Geomechanics, 22(6), 04022069. doi:10.1061/(asce)gm.1943-5622.0002320.

[70] Bateman, A. H., Crispin, J. J., Vardanega, P. J., & Mylonakis, G. E. (2022). Theoretical t-z Curves for Axially Loaded Piles. Journal of Geotechnical and Geoenvironmental Engineering, 148(7), 04022052. doi:10.1061/(asce)gt.1943-5606.0002753.

[71] Bohn, C., Lopes dos Santos, A., & Frank, R. (2017). Development of Axial Pile Load Transfer Curves Based on Instrumented Load Tests. Journal of Geotechnical and Geoenvironmental Engineering, 143(1), 04016081. doi:10.1061/(asce)gt.1943-5606.0001579.

[72] Zhou, Z., Zhang, Z., Chen, C., Xu, F., Xu, T., Zhu, L., & Liu, T. (2022). Application of load transfer method for bored pile in loess area. European Journal of Environmental and Civil Engineering, 26(10), 4457–4475. doi:10.1080/19648189.2020.1854125.

[73] Abchir, Z., Burlon, S., Frank, R., Habert, J., & Legrand, S. (2016). T-Z Curves for Piles from Pressuremeter Test Results. Geotechnique, 66(2), 137–148. doi:10.1680/jgeot.15.P.097.

[74] Xu, L. Y., Shao, W. Da, Xue, Y. Y., Cai, F., & Li, Y. Y. (2019). A simplified piecewise-hyperbolic softening model of skin friction for axially loaded piles. Computers and Geotechnics, 108, 7–16. doi:10.1016/j.compgeo.2018.12.018.

[75] Zhang, Q., Li, L., & Chen, Y. (2014). Analysis of Compression Pile Response Using a Softening Model, a Hyperbolic Model of Skin Friction, and a Bilinear Model of End Resistance. Journal of Engineering Mechanics, 140(1), 102–111. doi:10.1061/(asce)em.1943-7889.0000640.

[76] Li, L., Lai, N., Zhao, X., Zhu, T., & Su, Z. (2023). A generalized elastoplastic load-transfer model for axially loaded piles in clay: Incorporation of modulus degradation and skin friction softening. Computers and Geotechnics, 161, 105594. doi:10.1016/j.compgeo.2023.105594.

[77] Anoyatis, G., Mylonakis, G., & Tsikas, A. (2019). An analytical continuum model for axially loaded end-bearing piles in inhomogeneous soil. International Journal for Numerical and Analytical Methods in Geomechanics, 43(6), 1162–1183. doi:10.1002/nag.2886.

[78] Xia, Z., & Zou, J. (2017). Simplified Approach for Settlement Analysis of Vertically Loaded Pile. Journal of Engineering Mechanics, 143(11), 04017124–1. doi:10.1061/(asce)em.1943-7889.0001334.

[79] Liu, J., Xiao, H. B., Tang, J., & Li, Q. S. (2004). Analysis of load-transfer of single pile in layered soil. Computers and Geotechnics, 31(2), 127–135. doi:10.1016/j.compgeo.2004.01.001.

[80] Liu, Y., Jiang, S., Vanapalli, S. K., & Li, J. (2024). Mechanical Behavior of Pile Foundations Associated with Water Infiltration in Unsaturated Collapsible Soils. International Journal of Geomechanics, 24(6). doi:10.1061/ijgnai.gmeng-9279.

[81] Chong-fu, W. U., Wei-chao, G. U. O., Yu-nong, L. I., & Rui, T. I. E. (2016). Calculation of neutral surface depth and pile-soil stress ratio of rigid pile composite foundation considering influence of negative friction. Chinese Journal of Geotechnical Engineering, 38(2), 278-287. doi:10.11779/CJGE201602011. (In Chinese).

[82] Uge, B. U., Guo, Y., Zhao, J., Liu, Y., Li, Y., Hou, S., Lv, C., & Xia, Y. (2025). Load-transfer analysis of disconnected piled raft in unsaturated soils: Application and validation of the modified shear displacement method. Results in Engineering, 28. doi:10.1016/j.rineng.2025.107684.

[83] Cao, F., Ye, C., Wu, Z., Zhao, Z., & Sun, H. (2024). Settlement Calculation of Semi-Rigid Pile Composite Foundation on Ultra-Soft Soil under Embankment Load. Buildings, 14(7), 1954. doi:10.3390/buildings14071954.

[84] GB 50007-2011. (2011). Code for Design of Building Foundation. China National Standards, Beijing, China.